

Kosterlitz–Thouless transition in 1D Heisenberg antiferromagnet: An evidence based on topological properties of the ground state

Piotr Tomczak and Piotr Jabłoński

Faculty of Physics, ul. Umultowska 85, 61-614 Poznań, Poland

(Dated: February 3, 2017)

A Kosterlitz–Thouless phase transition in the ground state of an antiferromagnetic spin- $\frac{1}{2}$ Heisenberg chain with nearest and next-nearest-neighbor interactions is re-investigated from a new perspective: A mapping of the components of the scalar product onto a set of loops is found. One can classify these loops according to whether any two of them can be transformed into each other in a continuous way (i.e., whether they have the same winding number). A finite size scaling of the fidelity susceptibility and geometrical phase calculated within each class of above mentioned loops leads to the accurate critical coupling constant value and enables one to find that the critical exponent $\nu = 2.000 \pm 0.001$.

PACS numbers: 64.70.Tg, 05.30.Rt, 64.60.an, 75.10.Jm

Introduction. — At quantum phase transition (QPT) properties of the ground state of the quantum system change drastically due to quantum fluctuations which are most clearly pronounced at zero temperature. Although many approaches have been proposed to examine QPTs, to locate critical points and to calculate values of critical exponents, one still asks an important question: Is it possible to explore the critical behavior of a system at QPT by examining the change of its ground state $|\Psi_0\rangle$ in a critical region, especially when there is no possibility to identify an order parameter nor to establish a pattern related to a symmetry breaking? Still there exists, in this field, a quest for new approaches, based on scaling and renormalization, which enable searching and characterizing QPTs. Recently, mostly due to interplay between information theory and quantum many-body physics, new possibilities have been found for the studying of QPTs, see e.g., Refs. [1, 2].

The model under consideration and its essential properties. — An additional answer to the question raised in the *Introduction* is presented below result of reexamination of a quantum phase transition in the known^{3–5} one-dimensional spin- $\frac{1}{2}$ antiferromagnet with nearest (J_1) and next-nearest (J_2) neighbor interactions

$$H = J_1 \sum_i \mathbf{S}_i \mathbf{S}_{i+1} + J_2 \sum_i \mathbf{S}_i \mathbf{S}_{i+2}. \quad (1)$$

The ground state of this system depends on $\lambda = J_2/J_1$. Namely, for $\lambda < \lambda_c = 0.2411$ it exhibits the characteristics of a 1D antiferromagnet with nearest-neighbor interactions only (spin liquid phase), i.e., it is critical with correlations decaying $\propto \log(r)/r$ (r stands for spin-spin separation). Excitations are gapless - the finite-size triplet gap scales $\propto 1/L$ (also with log correction), with L being the chain length. For $\lambda > \lambda_c$ the system displays completely different ground state (dimerized phase): correlations decay exponentially and triplet gap remains open in thermodynamic limit. The transition between these phases is known to be of Kosterlitz–Thouless type.

Resonating Valence Bond (RVB) basis and winding numbers. — Examining this model in RVB basis sheds

additional light on its critical properties: it enables one to find the critical value of coupling constant and the critical exponent ν . Recall then, briefly, the essential features of RVB approach^{6,7} to quantum spin- $\frac{1}{2}$ systems: Matrix elements of the Hamiltonian are calculated not in the Ising basis but in the (complete) non-orthogonal basis $|c_k\rangle$ taken from an over-complete set of *singlet coverings*:

$$\langle c_k | \mathbf{S}_i \cdot \mathbf{S}_j | c_l \rangle = (-1)^d \left(\pm \frac{3}{4} \right) \langle c_k | c_l \rangle, \quad (2)$$

$\langle c_k | c_l \rangle = 2^{\mathcal{N}(c_k, c_l) - \mathcal{N}_s}$ with $\mathcal{N}(c_k, c_l)$ being a number of loops arising when the coverings $\langle c_k |$ and $|c_l\rangle$ are drawn simultaneously on the same lattice (“transition graph”) and $\mathcal{N}_s = \frac{L}{2}$ stands for the number of singlets in the system. All singlets belonging to $|c_k\rangle$ are oriented; d denotes the number of *disoriented* ones one meets while moving along the loop in $\langle c_k | c_l \rangle$ containing i and j . Finally, $+\frac{3}{4}$ is taken if there is even number of dimers between i to j , $-\frac{3}{4}$ in the opposite case. In order to find the ground state of Hamiltonian (1) one solves the generalized eigenproblem: $H|\Psi_0\rangle = E_0 C|\Psi_0\rangle$, with C being the matrix formed from scalar products $\langle c_k | c_l \rangle$.

Although, due to nonorthogonality, this procedure is a bit more burdensome from calculational point of view, it has a great advantage because of its clear meaning, especially when one uses periodic boundary conditions and maps the periodicity of the Hamiltonian onto a circle. Then one can characterize the ground state $|\Psi_0(\lambda)\rangle$, also by some *topological* properties in the following way. The scalar product, $\langle \Psi_0(\lambda) | \Psi_0(\lambda) \rangle$, can be interpreted as a set of loop coverings (transition graphs) of the lattice. One can define the winding number⁸ for a loop (in the plane, around a center of the circle which results from periodic boundary conditions) as an integer representing the number of times one encircles the center while moving along this loop. The winding number for a given transition graph is the largest winding number from the the winding numbers assigned to all loops forming this transition graph. An equivalent definition⁹ states that each loop from the transition graph can carry a „lattice flux”, which can be directly related to a winding number

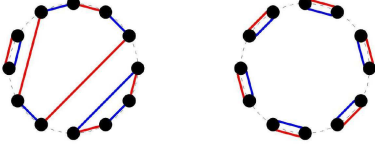


FIG. 1: Examples of representing scalar products $\langle c_k | c_l \rangle$ of two basis functions $|c_k\rangle$ (red) and $|c_l\rangle$ (blue) in a 12-spin system. The “transition graph” on the left is non contractible (contains 3 loops, absolute value of its winding number equals to 1, topological sector W1), whereas on the right is contractible (contains 6 loops, its winding number equals to 0, topological sector W0).

of this transition graph. In the case under consideration there exist two possibilities: absolute value of winding number equals to 0 (W0) or 1 (W1), see examples in Fig. 1. Consequently, each transition graph $\langle c_k | c_l \rangle$ may be classified according to its winding number. Two transition graphs with the same winding numbers belong to the same homotopy class, i.e., they can be transformed into each other in a continuous way.

The scalar product, the ground state energy and the derivatives of the scalar product in topological sectors. — Let us take into account that the ground state is normalized: $\langle \Psi_0(\lambda) | \Psi_0(\lambda) \rangle = 1$. Differentiating with respect to λ one obtains $\langle \partial_\lambda \Psi_0 | \Psi_0 \rangle = -\langle \Psi_0 | \partial_\lambda \Psi_0 \rangle$. Expressing the ground state in the RVB basis $|c_i\rangle$

$$|\Psi_0\rangle = \sum_i \alpha_i(\lambda) |c_i\rangle, \quad (3)$$

and taking into account that for the system under consideration all coefficients $\alpha_i(\lambda)$ may be chosen to be *real numbers*, leads to the conclusion that $\langle \partial_\lambda \Psi_0 | \Psi_0 \rangle = \langle \Psi_0 | \partial_\lambda \Psi_0 \rangle = 0$. (Another possibility is that it is purely imaginary. We examine the first possibility, the report on the second one — which leads to the same conclusions will be presented elsewhere). All the terms entering the scalar product (SP)

$$\langle \Psi_0 | \Psi_0 \rangle = \sum_{i,j} \alpha_i \alpha_j 2^{\mathcal{N}(c_i, c_j) - \mathcal{N}_s} \quad (4)$$

can be classified according to their *contractibility* (W0 or W1). This is also true for derivatives $\langle \partial_\lambda \Psi_0 | \Psi_0 \rangle$ and $\langle \Psi_0 | \partial_\lambda \Psi_0 \rangle$ since to calculate them one has to replace terms $\alpha_i \alpha_j$ in Eq. (4) by $\frac{\partial \alpha_i}{\partial \lambda} \alpha_j$ and $\frac{\partial \alpha_j}{\partial \lambda} \alpha_i$, respectively. The scalar product, $\langle \Psi_0(\lambda) | \Psi_0(\lambda) \rangle$, calculated for 24 spin system, split into two topological sectors, W0 and W1 is presented in Fig. 2. Note that contributions (from sectors W0 and W1) are symmetrical about the straight line $\frac{1}{2}$ and that for $\lambda = \frac{1}{2}$ (i.e., for the exact Majumdar-Gosh ground state) there are no non contractible loops in $\langle \Psi_0 | \Psi_0 \rangle$ — for finite L they decay $\propto 2^{-L/2}$. Let us stress that the probability of finding a “non contractible” term in the ground state monotonically tends to 0 as $\lambda \rightarrow \frac{1}{2}$.

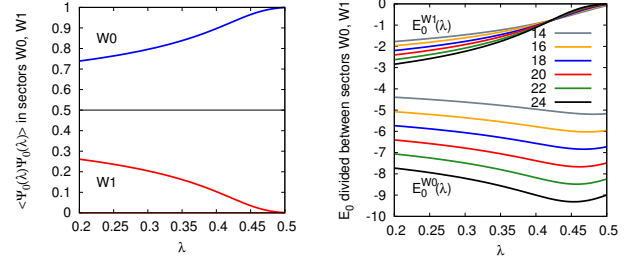


FIG. 2: Scalar product $\langle \Psi_0(\lambda) | \Psi_0(\lambda) \rangle$ in 24-spin system split between topological sectors W0 and W1 (left). The ground state energy $E_0(\lambda)$ divided into sectors W0 and W1 in systems up to 24 spins (right).

Considering the dependence of the GS energy E_0 on λ , one can also identify the contributions to the energy from the different topological sectors: $E_0 = \langle \Psi_0 | H | \Psi_0 \rangle = \langle \Psi_0 | H | \Psi_0 \rangle_{W0} + \langle \Psi_0 | H | \Psi_0 \rangle_{W1} = E_0^{W0}(\lambda) + E_0^{W1}(\lambda)$, see Fig. 2 (right). It follows that the GS energy of the system is associated with two types of topologically different objects: contractible and non contractible (cf. vortex-anti vortex pairs and vortices at the Kosterlitz-Thouless phase transition for classical 2D XY Heisenberg system) and there exists an energy gap ($\Delta E_0(\lambda) = E_0^{W1} - E_0^{W0}$) between non contractible objects and contractible ones. Growing λ raises the energy of non contractible objects and total GS energy and lowers the energy of contractible objects.

One can recall here the *energy-entropy* (Peierls) argument pointing that the interplay between contractible and non contractible objects leads to a topological phase transition in the system under consideration. Let us estimate how does the energy, $\Delta E_0(\tilde{\lambda})$ needed to create a non contractible object from a contractible one (i.e., to pass from W0 to W1 sector) depends on L . $\tilde{\lambda}$ stands for a *pseudocritical* value of λ which is calculated for an inflection point in the dependence $E_0^{W1}(\lambda)$ (Note that $\tilde{\lambda} \rightarrow \lambda_c$ for $L \rightarrow \infty$). The difference, $\Delta E_0(\tilde{\lambda})$, increases linearly with L : $\Delta E_0(\tilde{\lambda}) \propto 0.3088L$. The creation of a non contractible covering may be done approximately in $\frac{1}{2}C_{L/2}^2$ ways ($C_{L/2} = \frac{L!}{(L/2)!(L/2+1)!}$). One has

$$0.3088L - \lambda_c \log\left(\frac{1}{2}C_{L/2}^2\right) = 0, \quad (5)$$

and eventually, for large L , $\lambda_c = 0.223$ (which should be compared with 0.241).

Fidelity susceptibility and estimation of the critical properties of the system. — One can expect that the inflection points present in the scalar product $\langle \Psi_0 | \Psi_0 \rangle$ dependence on λ should result in extremes of its derivatives: $\langle \partial_\lambda \Psi_0 | \Psi_0 \rangle$ and $\langle \Psi_0 | \partial_\lambda \Psi_0 \rangle$ in both topological sectors. Indeed, numerical results show that the derivative (calculated numerically with an accuracy 10^{-8}) of SP with respect to λ exhibits a peak (see Fig. 3 - top left) located at $\lambda^*(L) > \lambda_c$.

Having determined the dependencies of the derivatives of the scalar product on λ , one can calculate the fidelity

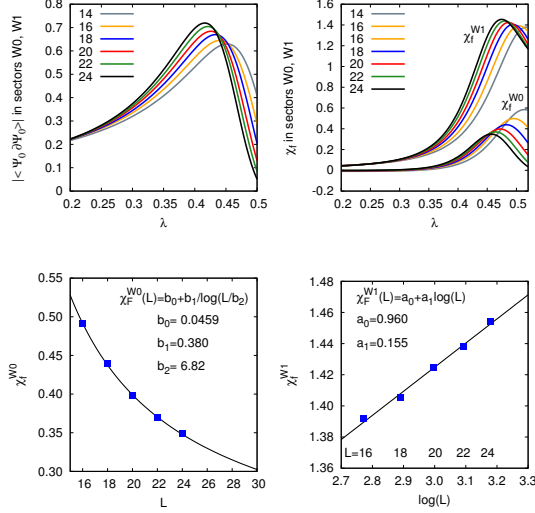


FIG. 3: The absolute value of the scalar product derivative $|\langle\Psi_0|\partial\Psi_0\rangle|$ with respect to λ in sectors W0 and W1 (top left) and the fidelity susceptibility per spin, $\frac{1}{L}\langle\partial\Psi_0|\partial\Psi_0\rangle$ (top right) in systems up to $L=24$ spins as a function of the parameter $\lambda = J_2/J_1$. The fidelity susceptibility peak heights as a function of L in the W0 sector (bottom left) and as a function of $\log(L)$ in the W1 sector (bottom right).

susceptibility (per spin),

$$\chi_f(\lambda) = \frac{1}{L}\langle\partial_\lambda\Psi_0|\partial_\lambda\Psi_0\rangle = \chi_f^{W0}(\lambda) + \chi_f^{W1}(\lambda), \quad (6)$$

where χ_f^{W0} and χ_f^{W1} stand for the fidelity susceptibility components from sector W0 and W1, see Fig. 3 - top right. One can observe quite different scaling of maximum of $\chi_f(\lambda)$ with respect to L in both topological sectors: χ_f^{W1} is logarithmically divergent ($\propto 0.155 \log(L)$), χ_f^{W0} for finite systems approaches its infinite-size value $b_0 = 0.0459 \pm 0.0473$ with a logarithmic size correction $\propto \frac{b_1}{\log(L/b_2)}$ with $b_1 = 0.380$, $b_2 = 6.82$. Thus, for $L \rightarrow \infty$ $\chi_f(\lambda)$ is logarithmically divergent. This differs from the results¹⁰ obtained for 1D XXZ Heisenberg spin- $\frac{1}{2}$ system with open boundary conditions (OBC), pointing that fidelity susceptibility does not diverge at Kosterlitz-Thouless QPT in 1D system and numerical results were interpreted as logarithmic finite-size scaling corrections. Let us stress that if we would examine the scaling of χ_f with respect to L without its splitting into topological sectors, we would have received also the finite value of χ_f for $L \rightarrow \infty$ with logarithmic size correction (like¹⁰ for OBC). This correction, $b_1/\log(L/b_2)$, is still present in the W0 sector. This means that while examining topological phase transitions it is better to use periodic boundary conditions since even for large systems with OBC it is very easy to confuse a logarithmic correction with a logarithmic growth of the peak.

In order to find λ_c and the critical exponent ν (for the

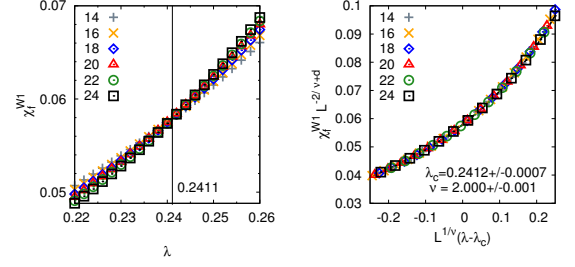


FIG. 4: Fidelity susceptibility in W1 sector before (left) and after rescaling (right) for systems with $L=16-24$ spins. The scaling collapse leads to the optimal values of λ_c and exponent ν . The errors were estimated by finding the collapse several times taking the numerical data with Gaussian noise with standard deviation equal to the accuracy of numerical differentiation.

correlation length) one takes into account an argument that $\chi_f^{W1}(\lambda)$, after appropriate rescaling of arguments and function values, for different system sizes should collapse onto the same curve. Let us assume^{1,11,12} that the fidelity susceptibility in the sector W1, at the critical point, scales as

$$\chi_f^{W1}(\lambda) = L^{2/\nu-d}\Phi(L^{1/\nu}(\lambda - \lambda_c)), \quad (7)$$

with Φ being a scaling function. The data from the left side of Fig. 4 has been plotted on the right side using rescaled values of argument $L^{1/\nu}(\lambda - \lambda_c)$ and function $\chi_f^{W1}(\lambda)L^{-2/\nu+d}$. The collapse occurs for $\lambda_c = 0.2412 \pm 0.0002$ and $\nu = 2.000 \pm 0.001$.

Relation to geometric phase. — It was shown that the derivative of the geometric phase calculated for the ground state of the quantum 1D XY model obeys scaling behavior in the vicinity of a quantum phase transition^{13,15}. In what follows a numerical argument is presented that the same is true for the the system under consideration and enables one to find its critical properties. Let us number the spins consecutively along the chain in such a way that odd (even) numbers are assign always to n.n.n. Now rotate spins on odd and even positions around the z direction by angles ϕ and $-\phi$, respectively. This defines a new, ϕ -dependent basis in which the spectrum of the Hamiltonian (1) remains unaltered. Under this transformation each singlet entering to a given basis function transforms as follows

$$|s\rangle = \frac{1}{\sqrt{2}}(|\uparrow\downarrow\rangle - |\downarrow\uparrow\rangle) \rightarrow |s'\rangle = \frac{1}{\sqrt{2}}(e^{i\frac{\phi}{2}}|\uparrow\downarrow\rangle - e^{-i\frac{\phi}{2}}|\downarrow\uparrow\rangle), \quad (8)$$

and the geometric phase, $\int \langle s' | \frac{\partial s'}{\partial \phi} \rangle d\phi$, for two spins- $\frac{1}{2}$ coupled antiferromagnetically in their ground state, due to equal contributions (with opposite sign) from the term $(e^{i\frac{\phi}{2}}|\uparrow\downarrow\rangle$ and the term $e^{-i\frac{\phi}{2}}|\downarrow\uparrow\rangle)$ equals to 0. The same is true for any finite system, but one can overcome this difficulty, by accumulating the geometric phase for only one term from Eq. (8) and similarly for larger systems.

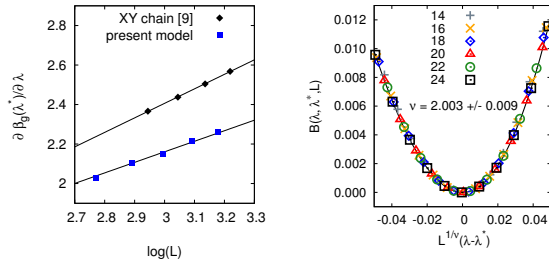


FIG. 5: The maximum value of the derivative $\frac{d\beta_g}{d\lambda}$ at the pseudocritical point λ^* (from Fig. 3 - top left), as a function of lattice size for the considered here system - squares and, for comparison, for the 1D spin- $\frac{1}{2}$ XY system - diamonds (left). The value of the function $B(\lambda, \lambda^*, L)$ defined by Eq. (9) versus $L^{1/\nu}(\lambda - \lambda^*)$ for system sizes $L = 16-24$. As expected from the finite size scaling ansatz the data for different system sizes collapse on a single curve for $\nu = 2.003$ (right). The error is estimated as explained in the caption of Fig. 4.

Eventually, the geometric phase, β_g , *per singlet*, for the ground state $|\Psi_0(\phi)\rangle$, accumulated by varying the angle ϕ from 0 to π is proportional to the $-i\pi\langle\Psi_0|\Psi_0\rangle$ and seems to be not λ -dependent one. The absolute value of its derivative, however, calculated in sectors W0 and W1 displays a well-marked peak at $\lambda^*(L) > \lambda_c$, which shifts towards λ_c with increasing L , see Fig. 3 (top left). The value of $\frac{d\beta_g}{d\lambda}$ calculated for $\lambda^*(L)$ diverges logarithmically with increasing L : $\frac{\partial}{\partial \lambda}\beta_g \propto 2.272 \log L$, see Fig. 5 (left). Similar dependence was reported¹³ for the ground state of the quantum XY chain, shown also in Fig. 5 (left). The logarithmic divergence suggests¹⁴ that it is also possible to extract a critical exponent ν from the scaling of the

function

$$B(\lambda, \lambda^*, L) = \left(1 - e^{\frac{d\beta_g(\lambda(L))}{d\lambda} - \frac{d\beta_g(\lambda^*(L))}{d\lambda}}\right) \propto L^{1/\nu}(\lambda(L) - \lambda^*(L)), \quad (9)$$

$\lambda^*(L)$ stands for the peak position for a given L (Fig. 3 - top left) and $\beta_g(\lambda(L))$ - for the geometric phase in the vicinity of λ_c for a given L . All the data for systems with different L collapse onto a single curve, see Fig. 5 (right), after taking $\lambda_c = 0.2411$ for $\nu = 2.003 \pm 0.009$.

Summary. — In this paper an example is given how to determine the values of critical couplings and critical exponent ν in a frustrated 1D spin system at topological quantum phase transition. The approach was based on finite size scaling of fidelity susceptibility and geometric phase; both quantities were calculated for different topological sectors. Topological sectors were defined taking into account contractibility of loops, existence of which is a natural consequence of the use of the RVB basis. This enabled to interpret the transition as a topological one and to find critical couplings and critical exponent ν for relatively small systems. We hope that the presented results will stimulate further exploration of critical phenomena in systems in which there is no possibility to define an order parameter.

Acknowledgments. — One of authors (PT) would like to thank Marcin Tomczak for stimulating discussions. This work was a part of a project financed by Narodowe Centrum Nauki (National Science Centre of Poland), Grant no. DEC-2011/03/B/ST2/01903. Numerical calculations were performed at Poznań Supercomputing and Networking Center under Grant no. 284.

- ¹ S.-J. Gu, *Fidelity Approach to Quantum Phase Transitions*, Int. J. Mod. Phys. B **24**, 4371 (2010).
- ² Lei Wang, Ye-Hua Liu, Jakub Imriska, Ping Nang Ma, and Matthias Troyer, *Fidelity Susceptibility Made Simple: A Unified Quantum Monte Carlo Approach*, Phys. Rev. X **5**, 031007 (2015), DOI: 10.1103/PhysRevX.5.031007.
- ³ Sebastian Eggert, *Numerical evidence for multiplicative logarithmic corrections from marginal operators*, Phys. Rev. B **54**, R9612 (1996).
- ⁴ Steven R. White, Ian Affleck, *Dimerization and incommensurate spiral spin correlations in the zigzag spin chain: Analogies to the Kondo lattice*, Phys. Rev. B **54**, 9862 (1996).
- ⁵ Anders W. Sandvik, *Computational Studies of Quantum Spin Systems*, arXiv:1101.3281v1, p. 101.
- ⁶ T. Oguchi, H. Kitatani, *Theory of Resonating Valence Bond Quantum spin system*, J. Phys. Soc. Jpn. **58**, 1403 (1989).
- ⁷ K. S. D. Beach, A. W. Sandvik, *Some formal results for the valence bond basis*, Nucl. Phys. B **750**, 142 (2006).
- ⁸ David J. Thouless, *Topological Quantum Numbers in Non-*

- relativistic Physics*, World Scientific Publishing, 1998, p. 12.
- ⁹ Ying Tang, Anders W. Sandvik, and Christopher L. Henley, *Properties of resonating-valence-bond spin liquids and critical dimer models*, Phys. Rev. B **84**, 174427 (2011).
- ¹⁰ G. Sun, A.K. Kolezhuk, and T. Vekua, *Fidelity at Berezinskii-Kosterlitz-Thouless quantum phase transitions*, Phys. Rev. B **91**, 014418 (2015).
- ¹¹ A. Polkovnikov, V. Gritsev, *Universal Dynamics Near Quantum Critical Points in Understanding Quantum Phase Transitions*, CRC Press, ISBN: 978-1-4398-0251-9.
- ¹² David Schwandt, Fabien Alet, and Sylvain Capponi, *Quantum Monte Carlo Simulations of Fidelity at Magnetic Quantum Phase Transitions* Phys. Rev. Lett. **103**, 170501 (2009).
- ¹³ Shi-Liang Zhu, *Scaling of Geometric Phases Close to the Quantum Phase Transition in the XY Spin Chain*, Phys. Rev. Lett. **96**, 077206 (2006).
- ¹⁴ M. N. Barber, *Finite Size Scaling in Phase Transitions and Critical Phenomena*, Eds. C. Domb and J. L. Lebowitz, Academic, 1983, Vol. 8.

- ¹⁵ Angelo C.M. Carollo and Jiannis K. Pachos, *Geometric Phases and Criticality in Spin-Chain Systems*, Phys. Rev. Lett. **95**, 157203 (2005).